Measurements of 4–10 keV x-ray production with the Z-Beamlet laser

L. E. Ruggles, J. L. Porter, P. K. Rambo, W. W. Simpson, M. F. Vargas, G. R. Bennett, and I. C. Smith

Citation: Review of Scientific Instruments **74**, 2206 (2003);
View online: https://doi.org/10.1063/1.1537854
View Table of Contents: http://aip.scitation.org/toc/rsi/74/3
Published by the American Institute of Physics

Measurements of 4–10 keV x-ray production with the Z-Beamlet laser

L. E. Ruggles,[a] J. L. Porter, Jr., P. K. Rambo, W. W. Simpson, and M. F. Vargas
Sandia National Laboratories, P.O. Box 5800, Albuquerque, New Mexico 87185-1193

G. R. Bennett
Ktech Corporation, Albuquerque, New Mexico 87106-4265

I. C. Smith
Atomic Weapons Establishment, Reading, Berkshire RG7 4PR, United Kingdom

(Presented on 11 July 2002)

In order to characterize the current backlighting capability of Sandia's Z-Beamlet laser (ZBL) over a range of high photon energies, we measured the x-ray conversion efficiency of the focused 527 nm ZBL beam into 4–10 keV x rays from He-like emission of the elements Sc through Ge (excluding Ga). The measurements approximated ZBL's nominal backlighting geometry and laser performance at Sandia's Z soft x-ray facility by irradiating planar foil targets several microns thick rotated 30° to the laser beam axis with a 600 ps pulse at 1 TW. The focal spot diameter was about 150 μm. This study includes measurements of the *K*-shell x-ray spectrum, x-ray power, and x-ray spot size with an array of filtered high-bandwidth silicon diodes, a convex LiF crystal spectrometer, step wedge filtered x-ray film, and a filtered x-ray pinhole camera. We found agreement with previous work for comparable laser parameters and recorded decreasing conversion efficiency versus atomic number and He-like photon energy. [DOI: 10.1063/1.1537854]

I. INTRODUCTION

The Z-Beamlet laser (ZBL),[1,2] a 2 TW, 2 kJ Nd:glass laser, was installed at Sandia National Laboratories, Albuquerque, in 2001. Z Beamlet was designed to be an x-ray backlighter for experiments on Sandia's Z,[3] a 20 MA, 100 ns rise-time pulsed power driver for z-pinch plasma radiation sources. Z is capable of generating pulses of up to 200 TW, 2 MJ sources of soft x rays.[4] These sources can be used as drivers for fusion experiments,[5–8] radiation effects testing, or complex hydrodynamics experiments. Z Beamlet was recently used to backlight inertial-confinement-fusion (ICF) experiments in which a target capsule located inside a two-sided secondary hohlraum was imploded using radiation from z pinches located on each side of the hohlraum.[5,7,9] These experiments used Ti and Fe laser targets to generate 4.7 and 6.7 keV x rays, respectively.

To measure the symmetry of ICF capsule experiments, 4–10 keV x rays are required to obtain adequate image contrast in radiograph images. To produce these x rays, the ZBL laser pulse is focused onto metal targets, forming a high temperature plasma that emits *K*-shell line radiation. The conversion efficiency of laser light to x radiation can vary with a number of parameters, including the laser wavelength, the pulse length, the surface irradiance, and target atomic number. Though a number of measurements have been made of x-ray yield and conversion efficiency for high power lasers,[10–12] for the parameters of the Z-Beamlet laser there are little data with which to compare. To support the ongoing backlighting experiments, we measured the intensity and spectral distribution of x rays produced using ZBL for a range of targets. In the few cases where the ZBL parameters were near those in the literature,[13] the data were directly compared.

II. DESCRIPTION OF EXPERIMENT AND DIAGNOSTICS

The ZBL pulse was nominally 1 TW for a 600 ps pulse at 2ω (527 nm) for these measurements. The pulse width was determined by recording the temporal width at half maximum of the injected pulse from the master oscillator and the 2ω beam energy was measured by using a calibrated calorimeter near the target chamber recording a known fraction of the total 2ω beam reflected from a wedge in the beamline. A 2 m focal length, 34-cm-square lens focused the laser energy into a 150–200-μm-diam spot on the target surface in an evacuated target chamber. The resulting laser irradiance at the focal spot was nominally $3-5\times10^{15}$ W/cm^2. The targets were 8–20-μm-thick pure planar metal foils mounted at the target chamber center with the target surface normal at $\theta=30°$ and $\phi=0°$ from the laser beam axis, where θ is the angle of azimuth and ϕ is the angle of elevation. A similar lens and target angle is used during backlighting experiments[7] with the base line final optics assembly on Z. The x-ray emission from the 11 elements Sc through Ge (excluding Ga) was characterized with a set of diagnostics viewing the target surface on a total of 17 shots.

A time-integrating, filtered pinhole camera recorded an image of the plasma source emission above 3500 eV. This image defined the focal spot size for these measurements. The instrument axis was aligned at $\theta=15°$, $\phi=-30°$ from target surface normal. The camera's pinhole, 5 μm diameter in a platinum substrate, was covered with 127 μm of polyimide and the camera's detector, Kodak 2492 film, was cov-

[a]Electronic mail: leruggl@sandia.gov

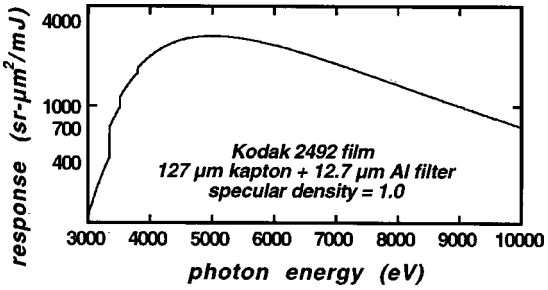

FIG. 1. Spectral response of the filtered pinhole camera. The sensitivity falls quickly below 3500 eV.

ered with 12.7 μm of aluminum. The pinhole was located 15.6 mm from the source and the image magnification was 8.16. The point source resolution (determined by the quadrature sum of the geometric pinhole projection, diffraction Airy disk diameter, and detector pixel sizes) of the instrument in this photon energy range is 6–7 μm for 21 μm pixel digitization of the image. The spectral sensitivity of the instrument with Kodak 2492 film is reasonably constant throughout the range of this study and very low for softer x rays (Fig. 1).

A convex curved crystal spectrometer, also time integrating, measured the *K*-shell emission from the target. The crystal, LiF(200) bent to a 69.85 mm radius on an aluminum alloy substrate, was mounted at 475 mm from the target and at $\theta=15°$, $\phi=45°$ from the target surface normal. Flat strips of 35 mm wide$\times$40 mm long Kodak 2492 and direct exposure film (DEF) recorded the spectra. The less sensitive 2492 was placed in front of the DEF, and both were covered with 127-μm-thick polyimide and 12.7-μm-thick aluminum filters. The crystal diffraction angle and the distance between the filtered film and the crystal were set for each target to include the $K\alpha$, He-like and H-like emission through the ionization potential of the H-like ion on the length of the film. A 51-μm-thick beryllium filter protected the instrument from debris and soft x rays.

An array of seven filtered silicon diodes measured the time-resolved x-ray flux from the target at $\theta=60°$, $\phi=30°$ from the target surface normal. The diodes, International Radiation Detector-type AXUV-HS1, have a 100 ps rise-time response[14] and the spectral response shown in Fig. 2 when the diode is apertured to expose only the active area to the source. All seven diodes were filtered with 50 μm of polyimide and 0.2 μm of aluminum, and six of the diodes had one through six additional 127 μm layers of polyimide. The

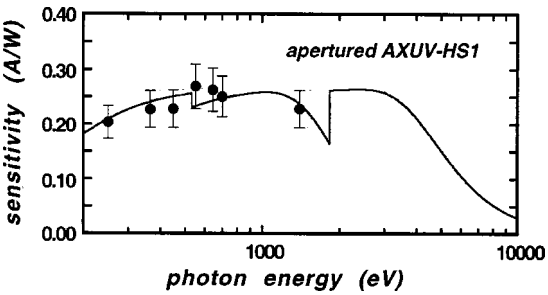

FIG. 2. Measured and calculated sensitivity of the unfiltered silicon diodes. The data points and error bars represent unpublished sensitivity measurements at Sandia by Ruggles and Simpson.

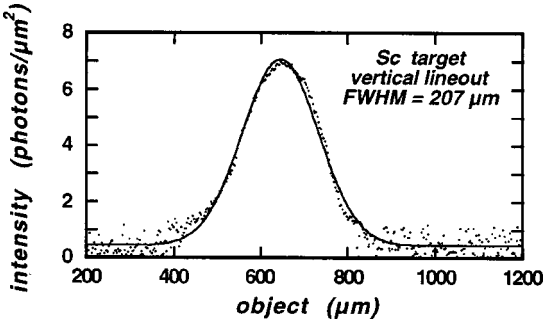

FIG. 3. Gaussian profile fit to a lineout through the center of the pinhole camera image of the Sc plasma.

signals were recorded on Tektronix TDS 694C digitizers at a system bandwidth greater than 1 GHz.

A film container with Kodak-types 2492 and 2497 film was mounted at 485 mm and $\theta=60°$, $\phi=0°$ from the target surface normal. The film was exposed to the source through a 112 step polyimide filter composed of seven rows of 127 μm steps and 16 columns of 50 μm steps. A 12.7-μm-thick aluminum filter covered the film to block visible light. The step wedge exposures were intended to separate spectral components of the source.

III. DATA REDUCTION TECHNIQUES AND RESULTS

The x-ray source size was determined by converting the scanned image on film recorded by the pinhole camera to x-ray intensity, plotting 42-μm-wide vertical and horizontal lineouts through the image and fitting the lineouts to a Gaussian function (Fig. 3). The full width at half maximum calculated by the Gaussian fits, corrected for the viewing angle of the pinhole camera and the instrument magnification, were averaged and are listed in Table I with the measured beam energy and the calculated laser irradiance on the target. We assumed the laser focal spot was the same size as the measured x-ray source size.

The convex crystal spectrometer (CCS) measured the conversion efficiency of the ZBL pulse into the He-like $1s^2-1s2p,s$ group of emission lines characteristic of the target. The CCS source flux measurement used published integrated LiF reflectivity[15] and film sensitivity.[16,17] The integrated reflectivity of the LiF crystal used for these measurements has not been measured, and this causes a large uncertainty, perhaps $\pm$50%, in our measured conversion efficiencies. The spectrometer was also inadequately baffled so that scattering of soft x rays in the instrument added an exposure to the films at the high photon energy end of the spectrum, especially for the higher atomic number targets where the film was nearer the line of sight to the target (see Fig. 4). The source intensity at the He-like lines was determined by using the method of Henke *et al.*[18] For a diffracting convex crystal, Henke relates the source intensity to the intensity within a given line profile as

$$i_0=N/\psi(d\chi/d\theta)R, \tag{1}$$

where $i_0=$the x-ray source energy (joules/sr), $N=$the total intensity recorded on film within the spectral line profile, $\psi=$the angle of source viewed by the crystal perpendicular to

TABLE I. Laser performance summary.

Target	2ω laser energy (joules)	Focal spot diameter (μm)	Laser irradiance (10^{15} W/cm^2)
Ge	632	165.1	4.86
Zn	672	149.2	6.33
Cu	396	174.4	2.73
Ni	621	202.4	3.18
Co	820	215.2	3.72
Fe	524	195.1	2.89
Mn	538	193.1	3.03
Cr	698	183.7	4.34
V	772	208.3	3.73
Ti	569	203.6	2.88
Sc	565	198.9	3.00

dispersion, $d\chi/d\theta=(r/s)\sin\theta$ where $r=$radius of crystal and $s=$source to crystal distance, $\theta=$the average Bragg diffraction angle, and $R=$the crystal coefficient of reflection. Using the technique of Phillion and Hailey,[13] we multiplied the measured source energy (joules/sr) by 4π (sr/sphere) and divided the result by the laser beam energy (joules) to determine the conversion efficiency ξ (joule/joule-sphere), implicitly assuming the source energy is radiated equally in all directions. The measured source energy is also corrected for the calculated transmission of the filters. The conversion efficiency determined by this method for the 11 elements is compared to similar measurements by Phillion and Hailey[13] in Fig. 5. The factor-of-2 error bars in the plot reflect our estimated uncertainty in the integrated reflectivity of the LiF crystal.

The DEF film saturated at the brightest peaks of the Cr and V spectra and the spectra recorded on the 2492 film was used to determine the DEF exposure by scaling for these two measurements.

The source intensity was also determined by a fit to the integrated silicon diode signals versus filter thickness. If the source is assumed to be emitting at two discrete photon energies, the signal from each diode can be described as

$$S=a_1\exp(-\mu_1\rho x)+a_2\exp(-\mu_2\rho x), \tag{2}$$

where ρ is the filter density, μ_n is the filter mass absorption coefficient at photon energy n, and x is the filter thickness. The intercepts $a_n=i_n/\eta_n\Omega$ contain the diode sensitivity η_n (A/W), the integrated diode signal i_n(A s), and the solid angle Ω (sr) subtended by the diode active area. For $n=1$ the photon energy is assumed to be the He-like $1s^2-1s2p,s$ group of emission lines characteristic of the target, thus defining μ_1 and leaving three unknowns (a_1, a_2, and μ_2) to be fit to the seven integrated diode signals (Fig. 6). This technique tends to separate the emission at the target *K*-shell energy from emission at other photon energies with the assumption that the source spectrum contains only two discrete energies. The residual photon energy is determined from μ_2. The results of this unfold are plotted in Fig. 7 on the same scale as Fig. 5 for comparison. We again show $\pm 50\%$ error bars to express the estimated uncertainty caused by forcing an unknown spectrum into two discrete photon energies.

The 2492 films exposed to the source through a step wedge were analyzed by an iterative fit. The spectral region from 4000 to 10 000 eV was grouped into 12 bins 500 eV wide that encompassed the *K*-shell radiation of each of the 11 target elements, and the exposure was calculated on each step of the step wedge for a guessed source spectral distribution. The calculated densities from each energy bin were summed (per Henke *et al.*[16,17]) for each step, the total calculated density for each step of the wedge was compared to the measured net density of each step and an appropriate adjust-

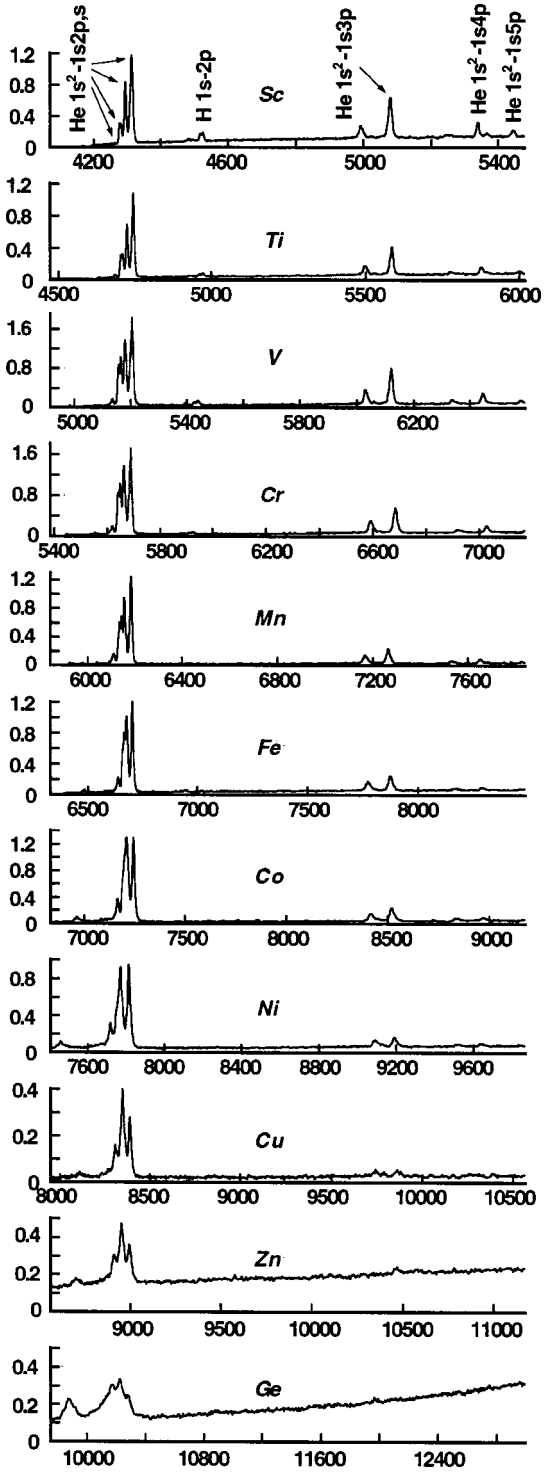

FIG. 4. Aligned plots of net diffuse density vs photon energy show the He-like emission decreasing for higher target Z. H-like emission is present only with low Z targets at the laser irradiance of this study.

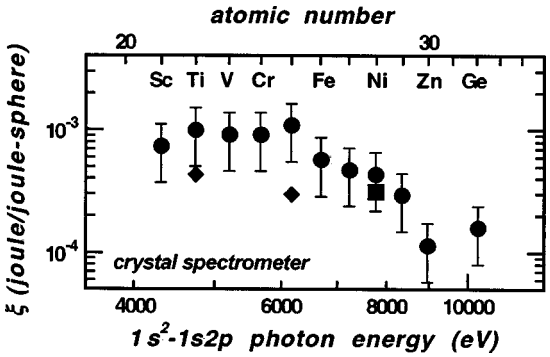

FIG. 5. Conversion efficiency (circles) measured with the convex crystal spectrometer for the He-like $1s^2-1s2p,s$ group of lines compared to Phillion *et al.* for 550 ps (square) and 125 ps (diamonds) laser pulses.

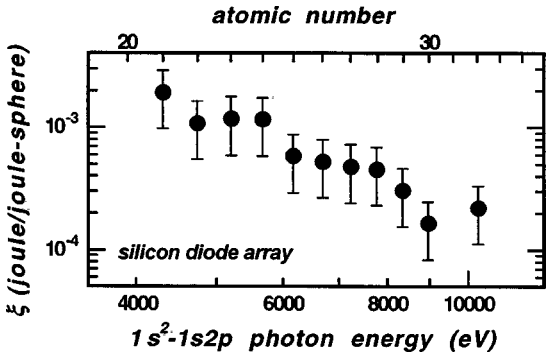

FIG. 7. Conversion efficiency measured with the silicon diode array for the He-like $1s^2-1s2p,s$ group of lines.

ment made to the input spectral distribution. The process was repeated until the errors reached a minimum. It was expected that the lower photon energy bins would affect the higher exposures from the thinner steps of the wedge and higher photon energy bins would affect the exposures at the thicker parts of the wedge. Unfortunately, the fits suggest a large contribution of energy above the spectral range of the calculation that seemed to remove much of the sensitivity of the fit to the energy distribution in the bins of interest. This effect occurred for most targets. Workman and Kyrala[19] encountered a similar problem with step wedge-filtered film on their scan of Fe, Zn, and Ge emission at the Omega laser. The most reasonable spectral fit was obtained for the Ti target and the spectral distribution (Fig. 8) for this shot does not indicate the high-photon-energy problem. When the energy bins were summed, however, the resulting total detected energy yield from most of the targets compared reasonably well to the total detected energy data from the other diagnostics (Fig. 9).

The x-ray source intensity was also estimated by integrating the total x-ray energy absorbed by the pinhole camera film. The source was assumed to be monochromatic at the He-like $1s^2-1s2p,s$ group of emission lines characteristic of the target and the film exposure converted to x-ray intensity using the film sensitivity measured by Henke.[16] Although the data obtained by this method have an error associated with the monochromatic source assumption, this total energy measurement agrees reasonably well with the other diagnostics for most of the targets (Fig. 9).

The films were developed according to Henke[16,17] and digitized with a HP 7490C scanner at 1200 dpi (21.2 μm/pixel). A Kodak calibrated diffuse density step wedge was scanned with each film and the resulting step wedge image reduced to a scanner response formula via a fit to the function.

$$\text{diffuse density} = a + b\tan(\text{cnts} - c_1) + d\tan(\text{cnts} - c_2), \quad (3)$$

where cnts = average scanner counts at each wedge and c_1 and c_2 are upper and lower rolloff constants. The scanner response was usable up to diffuse densities of 1.5. The images were converted to specular density (NA = 0.1) via the conversion ratio measured by Henke *et al.*,[16,17] and finally from specular density to intensity (photons per square micron) per Henke *et al.*[16,17]

IV. DISCUSSION

Using a variety of diagnostics, we have characterized the ZBL-produced *K*-shell emission from targets ranging from Sc to Ge (excluding Ga). The x-ray yields and conversion efficiencies obtained with different diagnostics agree to within the uncertainties for each diagnostic. The good agreement between film and silicon detectors, for example, suggests that the conversion efficiencies are accurate. In the few cases for which Phillion's data with the KMS *Chroma* laser[13] is close to the ZBL parameters, there is reasonably good agreement. The two shorter pulse data points in Fig. 5 from Phillion and Hailey would be expected to approach our results with a longer pulse at the same irradiance. We have also noted measurements by Molitoris *et al.*,[20] of He-like Zn thick target emission from *Nova 2-beam* produced plasmas.

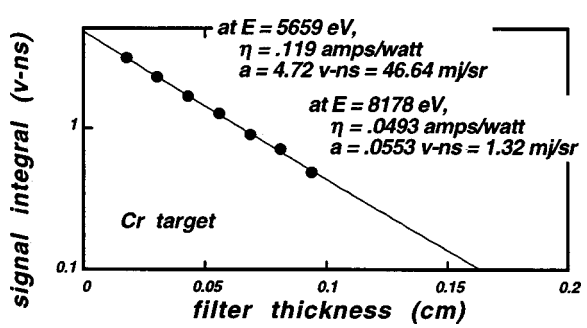

FIG. 6. Two-intercept fit to the time-integrated silicon diode signals acquired on the Cr target shot.

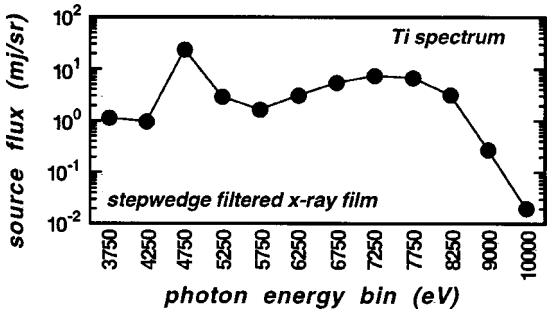

FIG. 8. Spectral unfold of the step wedge data for titanium. This is the best data obtained from the step wedge unfolds. Most of the fits returned an unreasonable spectrum with most of the flux in the high photon energy bins.

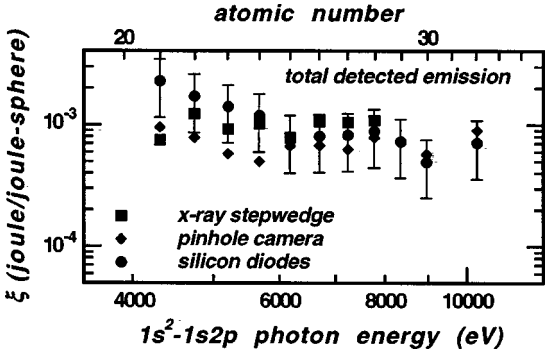

FIG. 9. Conversion efficiency to all detected photon energies measured with step wedge filtered film unfolds (squares), integrated pinhole camera film exposure (diamonds), and silicon diode array unfolds (circles and error bars). The sensitivity range of all three methods is limited to 3500–12 000 eV by filters and film or diode response.

For a target irradiance of about 4×10^{16} (a factor of 10 greater than this study) and a 100 ps pulse they measured a conversion efficiency of about 8×10^{-4} (almost a factor of 10 greater than this study). We have taken the liberty of integrating their published graphite crystal spectrometer data to calculate their conversion efficiency to He-like Zn.

Though the general trend in Fig. 9 is a decrease in efficiency with increasing atomic number (and *K*-shell photon energy), there is an apparent increase in the conversion efficiency when going from Zn to Ge. The crystal spectrometer data for Ge indicates an emission peak comparable to the He-like emission whose photon energy corresponds to Ge *K*-alpha radiation. A similar, but much smaller peak occurs in the Zn spectrum. The Ge *K*-alpha peak was included in the integration for the Ge conversion efficiency calculation and is likely responsible for the apparent increase in conversion efficiency to *K*-shell x rays (though a portion of the increase could be due to scattered radiation).

ACKNOWLEDGMENTS

These experiments would not have happened without the dedicated support of the Z-Beamlet staff, especially Robin Broyles, Mike Hurst, Antonio Garcia, Ben Thurston, and Chris Valleau. The authors thank John Beltran for carefully following the Burt Henke recipe for processing the film. This work was performed under the auspices of the United States Department of Energy by Sandia National Laboratories under Contract No. DE-AC04-94AL85000. Sandia is a multiprogram laboratory operated by Sandia Corporation, a Lockheed Martin Company.

[1] Advanced Conceptual Design Report for the Z-Beamlet Laser Backlighter System (UXRL-ID-134409), May 31, 1999.
[2] P. K. Rambo, J. L. Porter, Jr., G. R. Bennett, I. C. Smith, A. C. Erlandson, J. E. Murray, and J. Caird, in *OSA Trends in Optics and Photonics, Conference on Lasers and Electro-Optics* (Optical Society of America, Washington, DC, 2002), Vol. 73, pp. 362–363.
[3] M. K. Matzen, Phys. Plasmas **4**, 1519 (1997).
[4] R. B. Spielman, C. Deeney, and G. A. Chandler *et al.*, Phys. Plasmas **5**, 2105 (1998).
[5] M. E. Cuneo, R. A. Vesey, and J. L. Porter, Jr. *et al.*, Phys. Plasmas **8**, 2257 (2001).
[6] T. W. L. Sanford, R. E. Olsen, and R. L. Bowers *et al.*, Phys. Rev. Lett. **83**, 5511 (1999).
[7] G. R. Bennett *et al.*, (unpublished).
[8] D. L. Hanson, R. A. Vesey, and M. E. Cuneo *et al.*, Phys. Plasmas **9**, 2173 (2002).
[9] M. E. Cuneo, R. A. Vesey, and J. L. Porter, Jr. *et al.*, Phys. Rev. Lett. **88**, 215004 (2002).
[10] S. G. Glendinning, P. Amendt, K. S. Budil, B. A. Hammel, D. H. Kalantar, M. H. Key, O. L. Landen, B. A. Remington, and D. E. Desenne, *Applications of Laser Plasma Radiation II* (SPIE, Bellingham, WA, 1995), Vol. 2523, p. 29.
[11] R. Kauffman, in *Handbook of Plasma Physics*, Physics of Laser Plasmas, edited by A. M. Rubenchik and S. Witkowski (North-Holland, New York, 1991), Vol. 3.
[12] J. Workman and G. A. Kyrala, *Applications of X-rays Generated from Lasers and Other Bright Sources II* (SPIE, Bellingham, WA, 2001), Vol. 4504, p. 168.
[13] D. W. Phillion and C. J. Hailey, Phys. Rev. A **34**, 4486 (1986).
[14] G. C. Idzorek and H. Oona, Rev. Sci. Instrum. **68**, 1065 (1997).
[15] H. T. Yamada, B. L. Henke, and J. C. Davis (unpublished).
[16] B. L. Henke, F. G. Fujuwara, M. A. Tester, C. H. Dittmore, and M. A. Palmer, J. Opt. Soc. Am. B **1**, 828 (1984).
[17] B. L. Henke, J. Y. Uejio, G. F. Stone, C. H. Dittmore, and F. G. Fujuwara, J. Opt. Soc. Am. B **3**, 1540 (1986).
[18] B. L. Henke, H. T. Yamada, and T. J. Tanaka, Rev. Sci. Instrum. **54**, 1311 (1983).
[19] J. Workman and G. A. Kyrala, Rev. Sci. Instrum. **72**, 678 (2001).
[20] J. D. Molitoris, M. M. Morin, D. W. Phillion, A. L. Osterheld, R. E. Stewart, and S. D. Rothman, Rev. Sci. Instrum. **63**, 5104 (1992).